European Journal of Radiology 141 (2021) 109821

Contents lists available at ScienceDirect

European Journal of Radiology

journal homepage: www.elsevier.com/locate/ejrad

Heterogeneity of bone metastases as an important prognostic factor in patients affected by oestrogen receptor-positive breast cancer. The role of combined [18F]Fluoroestradiol PET/CT and [18F] Fluorodeoxyglucose PET/CT

Gianluca Bottoni [a,1], Arnoldo Piccardo [a,*,1], Francesco Fiz [a], Giacomo Siri [b], Federica Matteucci [c], Andrea Rocca [d], Oriana Nanni [e], Manuela Monti [e], Etienne Brain [f], Jean Louis Alberini [g], Bassam Dib [h], Gian Mauro Sacchetti [h], Chiara Saggia [i], Valentina Rossi [i], Nadia Harbeck [j], Rachel Wuerstlein [j], Tom Degenhardt [j], Andrea DeCensi [k], Gian Andrea Rollandi [l], Alessandra Gennari [m]

[a] Department of Nuclear Medicine, E.O. "Ospedali Galliera", Genoa, Italy
[b] Scientific Directorate, E.O. "Ospedali Galliera", Genoa, Italy
[c] Nuclear Medicine Unit Istituto Scientifico Romagnolo per lo studio e la cura dei tumori, IRST, Meldola, Italy
[d] Medical Oncology Unit Istituto Scientifico Romagnolo per lo studio e la cura dei tumori, IRST, Meldola, Italy
[e] Biostatistics and Clinical Trials Unit, Istituto Scientifico Romagnolo per lo studio e la cura dei tumori, IRST, Meldola, Italy
[f] Department of Clinical Research & Medical Oncology, Institut Curie (Hôpital René Huguenin), St Cloud, France
[g] Nuclear Medicine, Department Centre Georges-François Leclerc, 1 rue du Pr Marion, 21079 Dijon Cedex, France
[h] Nuclear Medicine Unit, AOU Maggiore della Carità, Novara, Italy
[i] Oncology Unit, AOU Maggiore della Carità, Novara, Italy
[j] Breast Centre, Department of Obstetrics and Gynaecology, University Hospital of Munich, Ludwig-Maximilians-University (LMU), Munich, Germany
[k] Department of Oncology, E.O. "Ospedali Galliera", Genoa, Italy
[l] Department of Radiology, E.O. "Ospedali Galliera", Genoa, Italy
[m] Department of Translational Oncology, University of Eastern Piedmont, Novara, Italy

ARTICLE INFO

Keywords:
Breast cancer
Bone metastases
Oestrogen receptor
Heterogeneity
^{18}F-FES
^{18}F-FDG

ABSTRACT

Purpose: To assess the prognostic role of different inter and intralesional expression (heterogeneity) of oestrogen receptor (ER) in bone metastases, as identified by the combined use of [18F]FES PET/CT and [18F]FDG PET/CT in patients with oestrogen receptor-positive (ER+) metastatic breast cancer (BC).

Methods: We analysed patients with a new diagnosis of bone metastases who were candidates for first-line systemic endocrine therapy. Before starting therapy, patients underwent baseline [18F]FES PET/CT and [18]FDG PET/CT. Semi-quantitative evaluation of whole-body bone metabolic burden (WB-B-MB) was performed on [18F]FES and [18F]FDG PET/CT in order to evaluate disease extent, tumour metabolism and ER heterogeneity. We used time-to-event analyses (Kaplan-Meier and Cox proportional-hazards methods) to estimate progression-free (PFS) and overall survival (OS), in order to assess the independent prognostic value of [18F]FES PET/CT and [18F]FDG PET/CT, alone and in combination.

Results: According to our criteria, we enrolled 49 patients. Over a median follow-up of 44.7 months, 35 patients suffered disease progression (71.4 %) and 15 died of disease (30.6 %). When the risk of disease progression was calculated by means of the Cox model, only [18F]FDG WB-B-MB was independently and directly associated to PFS ($p = 0.02$).

On analysing the association between all prognostic parameters and survival, the Cox model showed that the only parameter associated with OS was the WB-B-MB FES/FDG ratio ($p = 0.01$).

* Corresponding author at: Department of Nuclear Medicine, E.O. Ospedali Galliera, Mura delle Cappuccine 14, 16128 Genoa, Italy.
E-mail address: arnoldo.piccardo@galliera.it (A. Piccardo).
[1] The authors share co-authorship.

https://doi.org/10.1016/j.ejrad.2021.109821
Received 2 May 2021; Received in revised form 1 June 2021; Accepted 3 June 2021
Available online 10 June 2021

Conclusion: The combined use of [18F]FES-PET/CT and [18F]FDG-PET/CT can identify ER heterogeneity in BC bone metastases. This heterogeneity is significantly associated with survival. Moreover, the extension of the FDG-avid component correlates with the risk of disease progression.

1. Introduction

Bone metastases are a prominent cause of morbidity and mortality in cancer [1]. In particular, bone is the privileged metastatic location for endocrine-sensitive breast cancer (BC) [2–4]. Although the reasons for the preferential homing of BC cells towards the skeleton are still unclear, it seems plausible that bone marrow niches offer a suitable micro-environment for tumour survival [5,6]. Moreover, there is clinical evidence that BC expressing oestrogen receptors (ERs) has a higher tendency toward skeletal spread than other BC subtypes [7], which tend to colonize visceral organs [8].

In patients with endocrine-sensitive (ER+) BC, sensitive non-invasive biomarkers that can evaluate the presence and extension of bone metastases, together with their ER expression, are required. Indeed, approximately 70 % of BCs are considered endocrine-sensitive, on the basis of the expression of hormonal receptors on primary tumour.

However, endocrine therapy is effective in only about 50 % of ER + patients with metastases [9]. In this setting, the early identification of patients with ER + metastases who are not going to respond to endocrine therapy could avoid ineffective therapies and related toxicities, while prompting the earlier use of more efficacious treatments.

In recent years, [18F] Fluorine-oestradiol ([18F]FES) PET/CT has been proposed as an effective imaging procedure in detecting ER + metastases and predicting response to endocrine therapy [10]. Indeed, this whole-body imaging may provide excellent information about ER expression heterogeneity both within a given tumour and across multiple metastases in the same patient [11]. Although the sensitivity of [18F]FDG-PET/CT has proved higher than that of [18F] FES PET/CT, especially in the case of liver metastases [12–14], [18F] FES PET-CT is a reliable imaging procedure with high sensitivity especially in detecting bone metastases [12,13], guiding patient management [14] and predicting response to endocrine therapy [15]. In addition, in the particular setting of patients affected by invasive lobular carcinoma, which has indolent growth and low tumour glycolysis, [18F]

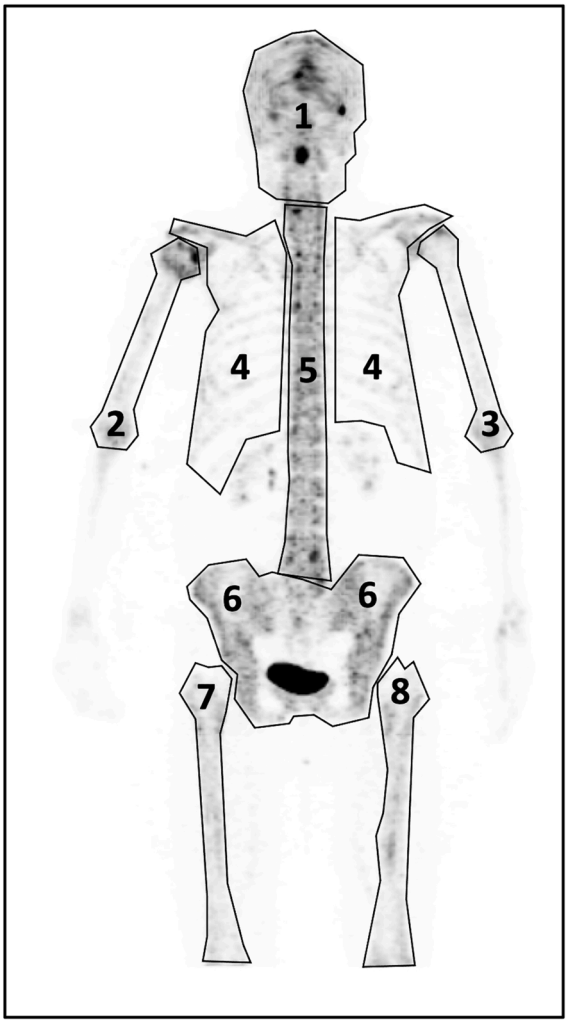

DE	SCORE
no involvment	0
one lesion	1
two lesions	2
three lesions	3
>3 foci or single diffuse lesion (<50% bone)	4
involvement 50-95% bone	5
involvement entire bone	6

FES	DE	SUVmean	MB (DE x SUVmean)
SKULL			
THORACIC CAGE			
R. HOMERUS			
L. HOMERUS			
SPINE			
PELVIS			
R: FEMUR			
L: FEMUR			
WB-B-MB (ΣB-MB)			

FDG	DE	SUVmean	MB (DE x SUVmean)
SKULL			
THORACIC CAGE			
R. HOMERUS			
L. HOMERUS			
SPINE			
PELVIS			
R: FEMUR			
L: FEMUR			
WB-B-MB (ΣB-MB)			

Fig. 1. The scoring system divides the skeleton into 8 anatomic segments. The disease extension (DE) score is graded as: 0, no sites per segment; 1, one discrete site per segment; 2, two discrete lesions; 3, three discrete lesions; 4, >3 discrete foci or a single lesion involving <50 % of a bone; 5, involvement of 50–95 % of the whole bone; 6, involvement of the entire bone (A). To obtain the bone metabolic burden (B-MB), we multiplied the highest mean standardized uptake value (SUVmean) by the DE of each bone segment. The whole-body bone metabolic burden (WB-B-MB) was calculated as the sum of the B-MB of each bone segment.

Table 1
Patients' characteristics.

N (%)	49 (100.0)
Age at onset of disease (years)	
mean (SD)	58.2 (13.0)
ER expression	
median (Q1–Q3)	80.0 (60.0–90.0)
Ki67 (%)	
median (Q1–Q3)	20.0 (10.0–25.0)
Visceral MTS, n(%)	
no	16 (32.7)
yes	33 (67.3)
FDG, n(%)	
neg	3 (6.1)
pos	46 (93.9)
SUV mean FDG	
median (Q1–Q3)	4.2 (3.2–5.5)
DE FDG	
median (Q1–Q3)	4.0 (2.0–16.0)
WB-B-MB FDG	
median (Q1–Q3)	17.6 (6.4–83.1)
FES, n(%)	
neg	7 (14.3)
pos	42 (85.7)
SUV mean FES	
median (Q1–Q3)	3.4 (1.8–4.9)
DE FES	
median (Q1–Q3)	5.0 (1.0–19.0)
WB-B-MB FES	
median (Q1–Q3)	13.3 (4.0–75.3)
WB-B-MB ratio FES/FDG	
median (Q1–Q3)	1.1 (0.4–2.1)

Note 1: SD = standard deviation; (Q1) = 1st quartile; (Q3) = 3rd quartile.

FES PET-CT can better reflect the metastatic burden than [18F] FDG-PET/CT [11,16].

Although, considerable inter- and intra-patient heterogeneity in [18F]FES uptake at different metastatic sites has been reported [13], no conclusive data on the association of positive [18F]FES PET/CT with progression-free survival (PFS) and overall survival (OS) are as yet available [17]. Therefore, [18F]FDG-PET/CT has been proposed as an additional tool to identify patients and metastases at higher risk of progression (i.e. low ER expression and high glycolytic activity).

The aim of our study was to assess the association between [18F]FES PET/CT and survival indices (i.e. PFS and OS) in ER-positive, Human Epidermal Growth Factor Receptor 2 (HER2)-negative BC patients with bone metastases undergoing endocrine therapy. We also aimed to evaluate the prognostic role of ER heterogeneity in bone metastases, as identified by the combined use of [18F]FES PET/CT and [18F]FDG PET/CT.

2. Materials and methods

2.1. Patients

We retrospectively analysed patients with a new diagnosis of bone metastases from ER-positive BC who were candidates for first-line endocrine therapy. Patients had been prospectively enrolled in a phase II multicentre international randomized clinical study (ET-FES JTC 2011 TRANSCAN project, EUDRACT number 2013-000287-29), the principal aim of which was to predict the efficacy of hormonal therapy in ER+, HER2- metastatic BC patients and validate the indication for [18F]FES PET/CT. The local ethics committees and the public medical agencies of the countries involved approved the study. All subjects provided written informed consent.

2.2. Imaging

At the baseline, all patients underwent [18F]FDG PET/CT and [18F] FES PET/CT within 10 days of each other; no treatment was administered between the two scans. Image acquisition was performed according to standard procedures [15,18].

Whole-body [18F]FDG PET/CT was carried out in fasting condition, 60 min after tracer injection. Data were acquired in the three-dimensional mode by means of dedicated PET/CT systems (the first Nuclear Medicine Department used Discovery ST, GE Medical Systems; the second used Discovery LS, GE Medical Systems; and the third Biograph mCT Flow, Siemens Medical Solutions). The activity administered was calculated according to the patient's body weight [18]. Whole-body [18F]FDG PET/CT images were acquired from the base of the skull to the mid-thigh and were reconstructed by means of an iterative algorithm. A non-diagnostic CT scan (low-dose CT with 120 kV, 80 mA) was used for attenuation correction and for anatomical localization of tracer uptake.

[18F]FES PET/CT acquisitions started 60 min after the injection of 200 MBq of [18F]FES. A low-dose CT-scan was used for attenuation correction in all patients. Patients were scanned from the base of the skull to the mid-thigh for 3 min per bed position [15].

Table 2
Factors influencing PFS.

	Incidence rate X 100 patients/ month	95 %CI	p-value
Overall	3.6	2.6–5.0	–
Age at onset of disease (years)			0.604
≤ 57	3.2	2.0–5.1	
> 57	4.0	2.5–6.4	
ER Expression			0.539
≤80.0	3.1	2.0–4.9	
> 80.0	4.3	2.7–7.1	
Ki67 (%)			0.528
≤ 20.0	4.1	2.7–6.2	
> 20.0	2.9	1.6–5.1	
Visceral MTS, n(%)			0.464
no	4.4	2.5–7.8	
yes	3.3	2.2–4.9	
FDG, n(%)			0.639
neg	2.1	0.5–8.3	
pos	3.7	2.7–5.3	
SUV mean FDG			0.148
≤ 4.2	2.9	1.7–4.7	
> 4.2	4.4	2.9–6.9	
DE FDG			0.123
≤ 4.0	2.7	1.6–4.4	
> 4.0	5.0	3.2–7.9	
WB-B-MB FDG			0.145
≤ 17.6	2.7	1.7–4.4	
> 17.6	5.0	3.2–7.8	
FES, n(%)			0.612
Neg	4.3	1.8–10.4	
Pos	3.5	2.4–5.0	
SUV mean FES			0.533
≤ 3.4	3.9	2.5–6.1	
> 3.4	3.2	1.9–5.3	
DE FES			0.663
≤ 5.0	3.2	2.1–5.1	
> 5.0	4.1	2.5–6.7	
WB-B-MB FES			0.665
≤ 13.3	3.9	2.5–6.2	
> 13.3	3.3	2.0–5.3	
WB-B-MB ratio FES/FDG			0.103
≤1.1	5.0	3.2–7.8	
> 1.1	2.6	1.6–4.3	

Note 1: Median follow-up (months) is calculated on the proportion of subjects who did not have disease progression: 42.3 months.
Note 2: qualitative variables are dichotomized by using the median value. Note 3: p-values are referred to log-rank test.

2.3. Scoring

The ability of [18F]FDG PET/CT and [18F]FES PET/CT to detect

Table 3
Factors influencing OS.

	Incidence rate X 100 patients/ month	95 %CI	p-value
Overall	0.9	0.5–1.5	–
Age at onset of disease (years)			0.460
<= 57	1.0	0.5–2.0	
> 57	0.7	0.3–1.6	
ER Expression			0.569
<= 80.0	0.8	0.4–1.6	
> 80.0	1.0	0.5–2.1	
Ki67 (%)			1.000
<= 20.0	0.9	0.5–1.7	
> 20.0	0.9	0.4–2.0	
Visceral MTS, n(%)			0.824
no	1.0	0.4–2.4	
yes	0.8	0.5–1.6	
FDG, n(%)			0.255
neg	0.0	–	
pos	1.0	0.6–1.6	
SUV mean FDG			0.925
<= 4.2	0.9	0.4–1.8	
> 4.2	0.9	0.5–1.8	
DE FDG			0.390
<= 4.0	0.7	0.3–1.5	
> 4.0	1.1	0.5–2.2	
WB-B-MB FDG			0.835
<= 17.6	0.8	0.4 –1.7	
> 17.6	0.9	0.4–2.0	
FES, n(%)			< 0.001
Neg	2.9	1.2–7.0	
Pos	0.7	0.4–1.2	
SUV mean FES			0.018
<= 3.4	1.4	0.8–2.4	
> 3.4	0.4	0.1–1.1	
DE FES			0.416
<= 5.0	1.0	0.6–1.9	
> 5.0	0.7	0.3–1.6	
WB-B-MB FES			0.307
<= 13.3	1.1	0.6–2.1	
> 13.3	0.7	0.3–1.5	
WB-B-MB ratio FES/FDG			0.005
<= 1.1	1.6	0.9–2.8	
> 1.1	0.3	0.1–1.0	

Note 1: qualitative variables are dichotomized by using the median value.
Note 2: p-values are referred to log-rank test.

breast cancer metastases was assessed by reviewing the uptake patterns of each radio-pharmaceutical. The mean standard uptake value (SUV-mean) of the bone lesions was recorded in each patient. A semi-quantitative scoring system was applied to [18F]FDG PET/CT and [18F]FES PET/CT, in order to evaluate disease extension. The skeletal distribution of each tracer was recorded in 8 segments: skull, thoracic cage, right humerus, left humerus, spine, pelvis, right femur and left femur (Fig. 1). The extent of skeletal involvement in each bone segment was scored on a 0–6 scale. Each segment was scored as previously validated [19] : 0 (no involvement), 1 (one discrete lesion), 2 (two discrete lesions), 3 (three discrete lesions), 4 (>3 discrete foci or a single diffuse lesion involving <50 % of a bone region), 5 (involvement of 50–95 % of a bone region), 6 (involvement of the entire bone region).

For both tracers, disease extension (DE) was calculated as the sum of the scores. To calculate the bone metabolic burden (B-MB), we multiplied the score of each segment by the SUVmean of a tumour isocontour, which was generated by setting the threshold at 40 % of the maximum SUV. The whole-body bone metabolic burden (WB-B-MB) was calculated as the sum of the B-MB [19]. In the case of a negative PET/CT result, the SUVmean, DE and WB-B-MB were assigned values of 1. [18F]FDG-PET/CT and [18F]FES-PET/CT images were interpreted after a consensus reading by two expert nuclear medicine physicians (GB and AP), who were aware of the patient's clinical history and of the results of morphological imaging modalities (MRI/CT).

To express a single score that took into account the results of both PET/CT scans in each patient, we finally calculated the ratio between the WB-B-MB of [18F]FES PET/CT and that of [18F]FDG PET/CT (WB-B-MB Ratio FES/FDG).

2.4. Treatment

All patients enrolled in this study received endocrine therapy, as clinically indicated [DOI: https://doi.org/10.1200/JCO.2016.67.1487]. However, the choice of agents was left to the clinical judgement of the treating physician, according to local clinical practice. Treatment was discontinued in the event of disease progression, unacceptable toxicity, patient refusal or decision of the treating physician.

2.5. Standard of reference

Follow-up based on contrast-enhanced CT and [18F]FDG PET/CT every 3 months served as the standard of reference for the final diagnosis of disease progression.

Disease progression was defined as an increase in the diameters of visceral metastases, according to the RECIST criteria [20], and/or the appearance of one or more new metastases [19,21]. Death due to disease was recorded when the patient's death was related to BC.

2.6. Statistical analysis

Descriptive statistics included mean, standard deviation, median, and 25th and 75th percentiles for continuous variables; in the case of categorical variables, absolute and relative values were used. Fisher's exact test and Kruskal-Wallis or t-tests were used to compare categorical and continuous variables, respectively. The Kaplan-Meier method was used to estimate the cumulative probability of PFS – defined as the interval between the initial diagnosis and the onset of progression of disease or death – and OS from the initial diagnosis to the date of death. A log-rank test was used to calculate differences between time-to-event curves. The Cox proportional-hazards model was used to estimate the risk of disease progression and death from any cause, after adjusting for the risk factors considered.

Since [18F]FDG PET/CT and [18F]FES PET/CT scores were highly correlated with WB-B-MB ratio (FES/FDG), in order to avoid collinearity, we used different models for each score, to test their independent association with PFS and OS. All analyses were conducted by means of Stata (version 14, StataCorp., College Station, TX, USA) software. Two-tailed probabilities are reported and a p-value of 0.05 was used to define nominal statistical significance.

3. Results

Of the 81 patients included in the ET-FES JTC 2011 TRANSCAN project, we retrospectively evaluated 49 according to our criteria. All 49 presented metastatic breast cancer (MBC) with ascertained bone involvement. All patients with visceral or soft tissue metastases without skeletal involvement were excluded. The principal characteristics of these patients are summarized in Table 1. [18F]FDG PET/CT identified bone metastases in 46 patients, and [18F]FES PET/CT in 42. However, all patients showed at least one positive bone metastasis on either [18F]FDG PET/CT or [18F]FES PET/CT. Six of the 7 patients with negative bone involvement on [18F]FES PET/CT also had FES-negative visceral metastases. All 3 patients with negative bone involvement on [18F]FDG PET/CT also had FDG-negative visceral metastases.

Over a median follow-up of 44.7 months (interquartile range = 35.2–48.2), 35 patients suffered disease progression (71.4 %) and 15 died of disease (30.6 %). Disease progression was observed in 33 of the 46 patients (71.7 %) with positive bone findings on [18F]FDG PET/CT and 15 (32.6 %) died of disease. Disease progression was

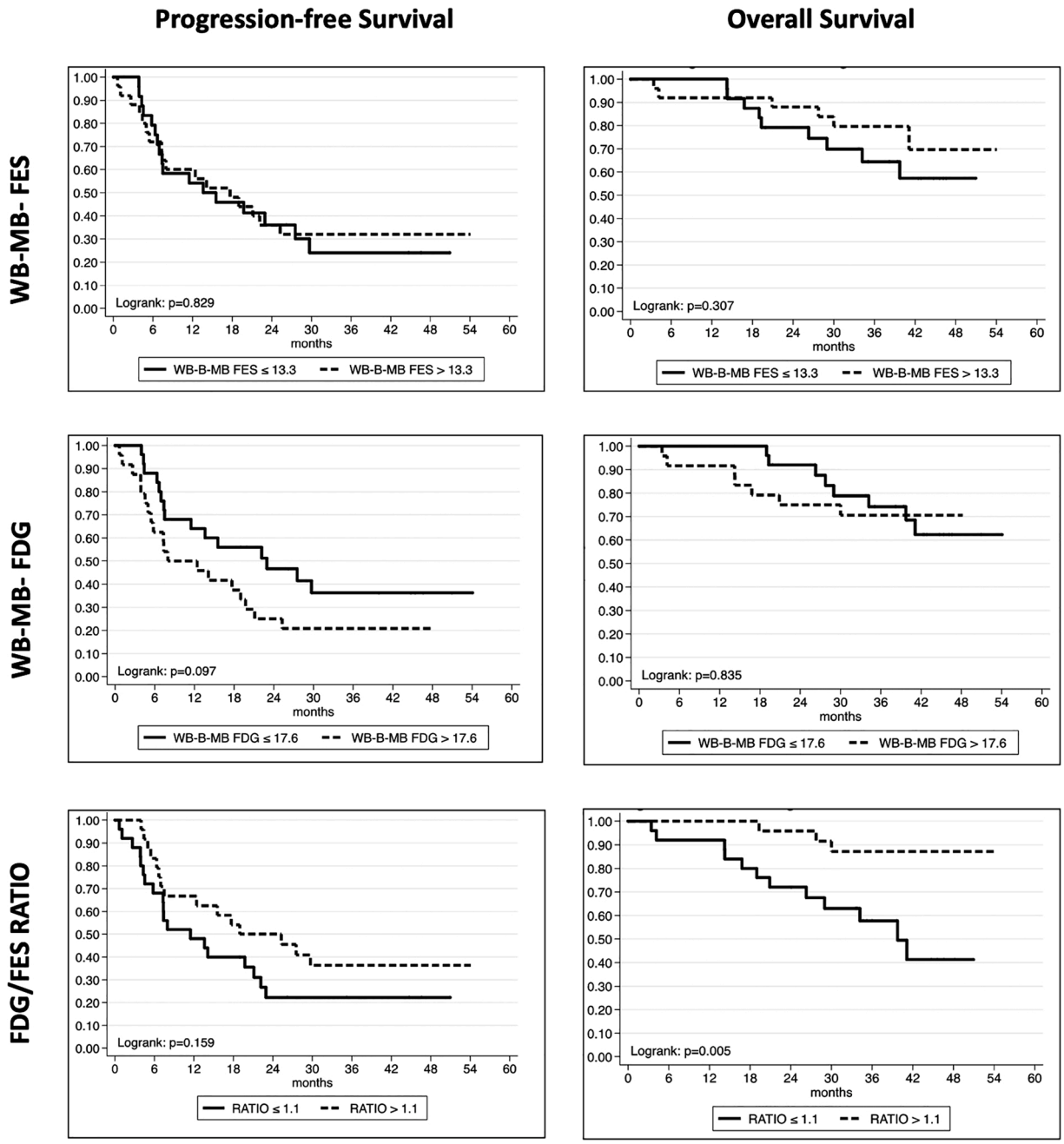

Fig. 2. Kaplan-Meier curves of progression-free survival and overall survival, stratified according to the median values of [18F]FDG-WB-B-MB and [18F]FES-WB-B-MB and the FES/FDG WB-B-MB Ratio).

Table 4
Cox Model for disease progression.

PFS	HR	P value	[95 % confidence interval]
WB-B-MB FDG (>17.6 vs ≤17.6)	3.56	0.022	1.21–11.53
WB-B-MB FES (>13.3 vs ≤13.3	0.34	0.055	0.11–1.03
Age at diagnosis	1.02	0.241	0.99–1.05
Estrogen receptor expression (%)	1.01	0.480	0.99–1.03
Ki67 (%)	1.01	0.527	0.97–1.05
Visceral Metastases (y/n)	1.03	0.949	0.48–2.21

observed in 30 of the 42 patients (71.4 %) with positive [18F]FES PET/CT and 10 (23.8 %) died of disease. None of the three [18F]FDG PET/CT-negative patients affected by documented bone metastases had died of disease by the end of follow-up. By contrast, 5 of the 7 patients with negative [18F]FES PET/CT and bone metastases had died of disease by the end of follow-up.

Factors influencing PFS and OS are summarized in Tables 2 and 3 respectively. Indeed, at univariate level, when the median value was considered as cut-off, no clinical or imaging risk factors influenced the PFS and only FES uptake and WB-B-MB ratio FES/FDG influenced the OS.

The association between all prognostic PET parameters and progression-free survival is shown by the Kaplan-Meier curves in Fig. 2.

In the multivariate analysis, according to the adjusted risk estimates for disease progression (Table 4), [18F]FDG-WB-B-MB proved directly associated to PFS. Specifically, patients with an [18F]FDG-WB-B-MB score >17.6 (median value) displayed a significantly higher risk of disease progression than those with an [18F]FDG-WBMB score ≤ 17.6 [HR = 3.56, 95 %CI = (1.21–10.53), p = 0.022]. Moreover, borderline

Table 5
A, Cox model for OS (WB-B-MB RATIO FES/FDG adjusted for WB-B-MB FDG and dichotomized by median); B, Cox model for OS (WB-B-MB RATIO FES/FDG adjusted for WB-B-MB FES and dichotomized by median).

Model A	HR	P value	[95 % confidence interval]
WB-B-MB Ratio FES/FDG (>1.1 vs≤1.1)	0.16	0.008	0.04–0.62
WB-B-MB FDG	1.00	0.600	0.99–1.01
Age at diagnosis	0.99	0.512	0.95–1.03
Estrogen receptor expression (%)	1.01	0.687	0.98–1.04
Ki67 (%)	1.01	0.674	0.95–1.08
Visceral Metastases (y/n)	1.29	0.672	0.39–4.27
Model B	**H.R.**	**P value**	**[95 % confidence interval]**
WB-B-MB Ratio FES/FDG (>1.1 vs≤1.1)	0.18	0.014	0.05–0.71
WB-B-MB FES	1.00	0.678	0.99–1.01
Age at diagnosis	0.99	0.512	0.95–1.03
Estrogen receptor expression (%)	1.01	0.742	0.97–1.04
Ki67 (%)	1.02	0.623	0.95–1.08
Visceral Metastases (y/n)	1.36	0.605	0.43–4.33

significance was observed in the association between [18F]FES-WB-B-MB and PFS, with a lower risk in patients with an [18F]FES-WB-B-MB value above the median (median = 13.3) [HR = 0.34, 95 %CI =(0.11–1.03), p = 0.055] (Table 4).

Kaplan-Meier curves for overall survival according to the prognostic factors are shown in Fig. 2. A significant association between FES/FDG WB-B-MB Ratio and OS was found (p = 0.01). This finding was confirmed by two multivariate Cox models on keeping the [18F]FDG-WB-B-MB (Table 5a) and F-FES-WB-B-MB (Table 5b) constant. It emerged that an FES/FDG ratio above the median (1.1) was associated with a lower risk of death [HR = 0.2, p = 0.01]. Fig. 3 depicts two examples of patients with opposing patterns of FDG and FES positivity.

4. Discussion

The present study investigated the biological substrate of susceptibility to endocrine treatment in patients with bone metastases originating from BC. Indeed, one possible explanation for the unpredictable response and/or acquired resistance to endocrine therapy is the heterogeneity of ER expression (i.e., the contemporary presence of metastases and cellular clones with different degrees of ER expression).

In our study, we focused our attention on patients with new evidence of bone metastases, and confirmed that pre-treatment molecular imaging with [18F]FES-PET/CT is a very effective aid to evaluating the inter-lesion heterogeneity of bone metastases in patients with ER + BC [12]. Indeed, when combined with [18F]FDG-PET/CT, [18F]FES-PET/CT proved to be a powerful prognostic biomarker that was able to identify those patients at higher risk of disease progression and death.

To quantify the heterogeneity of bone metastases on [18F]FES-PET/CT and [18F]FDG-PET/CT, we introduced a reproducible and easily obtainable parameter (i.e. WB-B-MB), which is able to simultaneously provide information on the extension of bone disease and on the intensity of tracer uptake. This index is able to capture the disease burden together with the rate of ER expression and glycolytic activity. To the best of our knowledge, no dedicated bone PET/CT scoring system has been developed that can correctly and automatically identify patients affected by bone metastases and stratify the risk of disease progression or death. The WB-B-MB is very easy to implement, can be calculated in every Nuclear Medicine Department, and has already been validated as a prognostic factor in patients with bone metastases [19,22].

By using the WB-B-MB, we confirmed that [18F]FDG-PET/CT was significantly associated with disease progression, high glycolytic activity often being the expression of high tumour grade and, more in general, of biological aggressiveness [19,23,24]. In addition, for the first time to our knowledge, we proved that the ratio between the WB-B-MB of FES and that of FDG could better quantify the heterogeneity of bone metastases and was the most powerful prognostic factor associated to OS when compared with the other clinical, histological and imaging parameters. Indeed, we found that the lower this WB-B-MB Ratio was (i.e <1.1) the higher the probability of dying of disease was.

Although [18F]FES-PET/CT has proved effective as a predictor of response to endocrine therapy, particularly in those with evidence of high oestrogen receptor density [11,25–29], little can be said about its prognostic role, especially in patients with bone lesions. One study evaluated this issue, but no conclusive results concerning the prognostic role of [18F]FES-PET/CT were reported [17]. A previous paper, however, reported that the density of ER expression was influenced by the treatment scheme: in a single-case report, a drop in ER expression was observed after first-line tamoxifen/anastrazole; this was followed by a

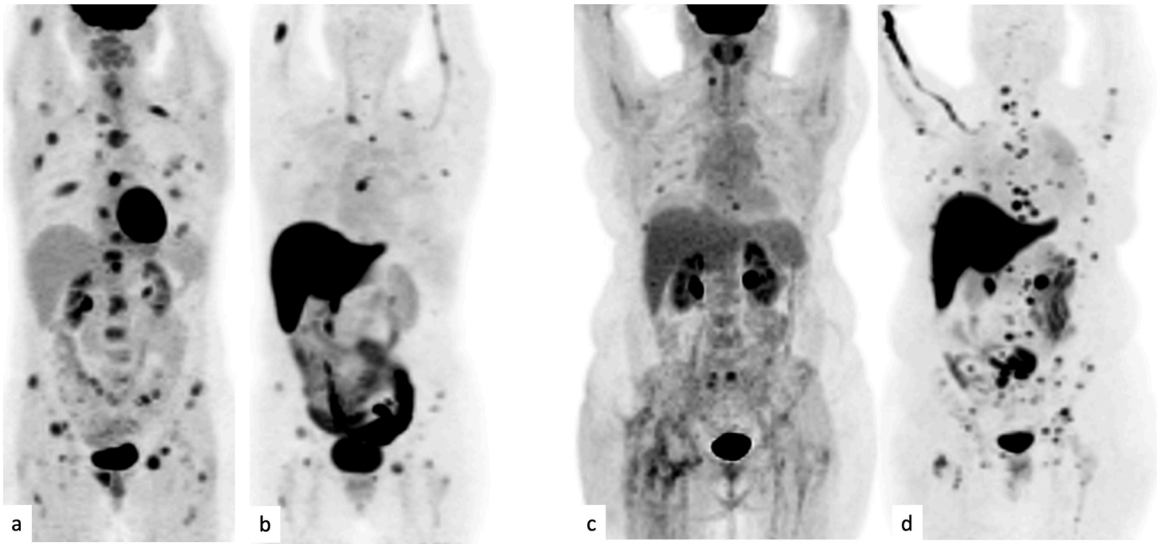

Fig. 3. 53-year-old woman affected by ER + BC bone metastases. [18F]FDG PET/CT (a) detected more bone metastases than [18F]FES PET/CT (b); the FES/FDG WB-B-MB ratio calculated was 0.79. The patient suffered disease progression and died of disease 20 months later. 60-year-old woman affected by ER + BC bone metastases. [18F]FDG PET/CT (c) detected fewer bone metastases than [18F]FES PET/CT (d); the FES/FDG WB-B-MB ratio calculated was 3.7. The patient did not suffer disease progression over time (i.e. 37 months) and is still alive.

resurgence when the patient was switched to cytotoxic treatment [30]. This finding allowed a further therapeutic switch from chemotherapy to a second-line hormone therapy, which was effective in achieving a response. Albeit isolated, this report might provide a key to interpreting the lack of association between FES expression and survival: the receptor profile appears to be dynamic and influenced by the hormonal treatment, which induces an internalization of ER and selects those cells without hormone receptor expression. Therefore, when trying to discern a correlation between FES PET and survival parameters, multiple time-points could be needed. Accordingly, in our study we did not find any significant correlation between [18F]FES-PET/CT-associated parameters (DE and WB-B-MB) and OS. However, we found that, by combining the information derived from [18F]FES-PET/CT with that yielded by [18F]FDG-PET/CT, we could obtain a reliable parameter, i.e. the FES/FDG WB-B-MB ratio, that could estimate the heterogeneity of bone metastases and therefore predict outcome.

Although our results are encouraging, some limitations should be borne in mind. First, this study was performed in a relatively limited number of patients, and the data were retrospectively analysed. However, all patients were prospectively enrolled in a clinical trial that only included ER+, HER 2-negative MBC patients with a new diagnosis of distant metastases. In this setting, the risk of selection bias seems to be limited.

Second, three different PET/CT scanners in three different Nuclear Medicine Departments were used to acquire PET images. Thus, the SUV of one PET/CT scanner might not be comparable to that of another, as the SUV is affected by the intrinsic characteristics of each PET/CT scanner. However, we used the same acquisition protocol and parameters in all three Nuclear Medicine Departments. Moreover, since instrument assessment and quality control measures are critical to interpreting quantitative PET data, phantom acquisition images were previously collected in two of the three imaging centres, in order to set up the PET/CT scanners.

Third, in the case of [18F]FES-PET/CT, the determination of WB-B-MB might not fully capture intra-patient and intra-metastatic heterogeneity in ER expression. This issue could be tackled by applying textural analysis to these images, in order to obtain information on the heterogeneity of the tissue.

5. Conclusion

Semi-quantification of [18F]FES-PET/CT and [18F]FDG-PET/CT performed at the time of first diagnosis of bone lesions in ER + BC patients is easy to perform and can identify the grade of metastatic heterogeneity, thereby providing important prognostic information in terms of OS.

CRediT authorship contribution statement

G. Bottoni: contributed to the conception of the study, acquired and analyzed data, drafting the manuscript. **A. Piccardo:** contributed to the conception of the study, acquired and analyzed data, drafting the manuscript. **G Siri:** contributed to the conception of the study, analyzed data, drafting the manuscript. **F. Matteucci:** contributed to the conception of the study and drafted the manuscript. **A. Rocca:** contributed to the conception and design of the study and drafted the manuscript. **O. Nanni:** contributed to the acquisition and analysis of data. **M. Monti:** contributed to conception of the study and analyzed data. **F. Fiz:** contributed to design of the study and revised the manuscript. **A. De Censi:** contributed to design the study and revised the manuscript. **E. Brain:** contributed to the acquisition and analysis of data. **JL. Alberini:** contributed to the acquisition and analysis of data. **B. Dib:** contributed to the acquisition and analysis of data. **M. Sacchetti:** contributed to the acquisition and analysis of data. **C. Saggia:** contributed to the acquisition and analysis of data. **V. Rossi:** contributed to the acquisition and analysis of data. **N. Harbeck:** contributed to design the study and revised the manuscript. **Rachel Wuerlestein:** contributed to design the study and revised the manuscript. **Tom Degenhard:** contributed to design the study and revised the manuscript. **A. Gennari:** revised the manuscript critically for important intellectual content.

Declaration of Competing Interest

The authors have no conflicts of interest.

Acknowledgements

This research received grants from “Associazione Italiana per la Ricerca sul Cancro” (AIRC 2013) and ERA-Net TRANSCAN JTC 2011 Italian Ministry of Health.

References

[1] R.E. Coleman, Clinical features of metastatic bone disease and risk of skeletal morbidity, Clin. Cancer Res. 12 (20 Pt 2) (2006) 6243s–6249s.
[2] G.R. Mundy, Metastasis to bone: causes, consequences and therapeutic opportunities, Nat. Rev. Cancer 2 (8) (2002) 584–593.
[3] M. Futakuchi, K. Fukamachi, M. Suzui, Heterogeneity of tumor cells in the bone microenvironment: mechanisms and therapeutic targets for bone metastasis of prostate or breast cancer, Adv. Drug Deliv. Rev. 99 (Pt B) (2016) 206–211.
[4] S.G. Wu, J.Y. Sun, L.C. Yang, L.Y. Tang, X. Wang, X.T. Chen, G.H. Liu, H.X. Lin, Q. Lin, Z.Y. He, Patterns of distant metastasis in Chinese women according to breast cancer subtypes, Oncotarget 7 (30) (2016) 47975–47984.
[5] T. Yoneda, T. Hiraga, Crosstalk between cancer cells and bone microenvironment in bone metastasis, Biochem. Biophys. Res. Commun. 328 (3) (2005) 679–687.
[6] T. Yoneda, P.J. Williams, T. Hiraga, M. Niewolna, R. Nishimura, A bone-seeking clone exhibits different biological properties from the MDA-MB-231 parental human breast cancer cells and a brain-seeking clone in vivo and in vitro, J. Bone Miner. Res. 16 (8) (2001) 1486–1495.
[7] C. Yeung, J. Hilton, M. Clemons, S. Mazzarello, B. Hutton, F. Haggar, C.L. Addison, I. Kuchuk, X. Zhu, K. Gelmon, A. Arnaout, Estrogen, progesterone, and HER2/neu receptor discordance between primary and metastatic breast tumours-a review, Cancer Metastasis Rev. 35 (3) (2016) 427–437.
[8] S.J. Lee, S. Park, H.K. Ahn, J.H. Yi, E.Y. Cho, J.M. Sun, J.E. Lee, S.J. Nam, J. H. Yang, Y.H. Park, J.S. Ahn, Y.H. Im, Implications of bone-only metastases in breast cancer: favorable preference with excellent outcomes of hormone receptor positive breast cancer, Cancer Res. Treat. 43 (2) (2011) 89–95.
[9] N. Harbeck, A. Rody, Lost in translation? Estrogen receptor status and endocrine responsiveness in breast cancer, J. Clin. Oncol. 30 (7) (2012) 686–689.
[10] M. van Kruchten, E.G.E. de Vries, M. Brown, E.F.J. de Vries, A. Glaudemans, R. Dierckx, C.P. Schroder, G.A.P. Hospers, PET imaging of oestrogen receptors in patients with breast cancer, Lancet Oncol. 14 (11) (2013) e465–e475.
[11] B.F. Kurland, J.R. Wiggins, A. Coche, C. Fontan, Y. Bouvet, P. Webner, C. Divgi, H. M. Linden, Whole-body characterization of estrogen receptor status in metastatic breast cancer with 16alpha-18F-fluoro-17beta-estradiol positron emission tomography: meta-analysis and recommendations for integration into clinical applications, Oncologist 25 (10) (2020) 835–844.
[12] M. van Kruchten, A.W. Glaudemans, E.F. de Vries, R.G. Beets-Tan, C.P. Schroder, R. A. Dierckx, E.G. de Vries, G.A. Hospers, PET imaging of estrogen receptors as a diagnostic tool for breast cancer patients presenting with a clinical dilemma, J. Nucl. Med. 53 (2) (2012) 182–190.
[13] H.H. Nienhuis, M. van Kruchten, S.G. Elias, A. Glaudemans, E.F.J. de Vries, A.H. H. Bongaerts, C.P. Schroder, E.G.E. de Vries, G.A.P. Hospers, (18)F-fluoroestradiol tumor uptake is heterogeneous and influenced by site of metastasis in breast cancer patients, J. Nucl. Med. 59 (8) (2018) 1212–1218.
[14] M. Gupta, A. Datta, P.S. Choudhury, M. Dsouza, U. Batra, A. Mishra, Can (18)F-fluoroestradiol positron emission tomography become a new imaging standard in the estrogen receptor-positive breast cancer patient: a prospective comparative study with (18)F-fluorodeoxyglucose positron emission tomography? World J. Nucl. Med. 16 (2) (2017) 133–139.
[15] M. van Kruchten, A. Glaudemans, E.F.J. de Vries, C.P. Schroder, E.G.E. de Vries, G. A.P. Hospers, Positron emission tomography of tumour [(18)F]fluoroestradiol uptake in patients with acquired hormone-resistant metastatic breast cancer prior to oestradiol therapy, Eur. J. Nucl. Med. Mol. Imaging 42 (11) (2015) 1674–1681.
[16] M.P. Hogan, D.A. Goldman, B. Dashevsky, C.C. Riedl, M. Gonen, J.R. Osborne, M. Jochelson, C. Hudis, M. Morrow, G.A. Ulaner, Comparison of 18F-FDG PET/CT for systemic staging of newly diagnosed invasive lobular carcinoma versus invasive ductal carcinoma, J. Nucl. Med. 56 (11) (2015) 1674–1680.
[17] B.F. Kurland, L.M. Peterson, J.H. Lee, E.K. Schubert, E.R. Currin, J.M. Link, K. A. Krohn, D.A. Mankoff, H.M. Linden, Estrogen receptor binding (18F-FES PET) and glycolytic activity (18F-FDG PET) predict progression-free survival on endocrine therapy in patients with ER+ breast cancer, Clin. Cancer Res. 23 (2) (2017) 407–415.
[18] R. Boellaard, R. Delgado-Bolton, W.J. Oyen, F. Giammarile, K. Tatsch, W. Eschner, F.J. Verzijlbergen, S.F. Barrington, L.C. Pike, W.A. Weber, S. Stroobants, D. Delbeke, K.J. Donohoe, S. Holbrook, M.M. Graham, G. Testanera, O.S. Hoekstra, J. Zijlstra, E. Visser, C.J. Hoekstra, J. Pruim, A. Willemsen, B. Arends, J. Kotzerke,

A. Bockisch, T. Beyer, A. Chiti, B.J. Krause, M. European Association of Nuclear, FDG PET/CT: EANM procedure guidelines for tumour imaging: version 2.0, Eur. J. Nucl. Med. Mol. Imaging 42 (2) (2015) 328–354.

[19] A. Piccardo, M. Puntoni, S. Morbelli, M. Massollo, F. Bongioanni, F. Paparo, V. Altrinetti, R. Gonella, A. Gennari, M. Iacozzi, G. Sambuceti, A. DeCensi, 18F-FDG PET/CT is a prognostic biomarker in patients affected by bone metastases from breast cancer in comparison with 18F-NaF PET/CT, Nuklearmedizin 54 (4) (2015) 163–172.

[20] E.A. Eisenhauer, P. Therasse, J. Bogaerts, L.H. Schwartz, D. Sargent, R. Ford, J. Dancey, S. Arbuck, S. Gwyther, M. Mooney, L. Rubinstein, L. Shankar, L. Dodd, R. Kaplan, D. Lacombe, J. Verweij, New response evaluation criteria in solid tumours: revised RECIST guideline (version 1.1), Eur. J. Cancer 45 (2) (2009) 228–247.

[21] S. Basu, W. Chen, J. Tchou, A. Mavi, T. Cermik, B. Czerniecki, M. Schnall, A. Alavi, Comparison of triple-negative and estrogen receptor-positive/progesterone receptor-positive/HER2-negative breast carcinoma using quantitative fluorine-18 fluorodeoxyglucose/positron emission tomography imaging parameters: a potentially useful method for disease characterization, Cancer 112 (5) (2008) 995–1000.

[22] A. Piccardo, G. Morana, M. Puntoni, S. Campora, S. Sorrentino, P. Zucchetta, M. Ugolini, M. Conte, A. Cistaro, G. Ferrarazzo, M. Pescetto, M. Lattuada, G. Bottoni, A. Garaventa, L. Giovanella, E. Lopci, Diagnosis, treatment response, and prognosis: the role of (18)F-DOPA PET/CT in children affected by neuroblastoma in comparison with (123)I-mIBG scan: the first prospective study, J. Nucl. Med. 61 (3) (2020) 367–374.

[23] S. Ueda, H. Tsuda, H. Asakawa, T. Shigekawa, K. Fukatsu, N. Kondo, M. Yamamoto, Y. Hama, K. Tamura, J. Ishida, Y. Abe, H. Mochizuki, Clinicopathological and prognostic relevance of uptake level using 18F-fluorodeoxyglucose positron emission tomography/computed tomography fusion imaging (18F-FDG PET/CT) in primary breast cancer, Jpn. J. Clin. Oncol. 38 (4) (2008) 250–258.

[24] G.A. Ulaner, A. Eaton, P.G. Morris, J. Lilienstein, K. Jhaveri, S. Patil, M. Fazio, S. Larson, C.A. Hudis, M.S. Jochelson, Prognostic value of quantitative fluorodeoxyglucose measurements in newly diagnosed metastatic breast cancer, Cancer Med. 2 (5) (2013) 725–733.

[25] J.E. Mortimer, F. Dehdashti, B.A. Siegel, J.A. Katzenellenbogen, P. Fracasso, M. J. Welch, Positron emission tomography with 2-[18F]Fluoro-2-deoxy-D-glucose and 16alpha-[18F]fluoro-17beta-estradiol in breast cancer: correlation with estrogen receptor status and response to systemic therapy, Clin. Cancer Res. 2 (6) (1996) 933–939.

[26] H.M. Linden, S.A. Stekhova, J.M. Link, J.R. Gralow, R.B. Livingston, G.K. Ellis, P. H. Petra, L.M. Peterson, E.K. Schubert, L.K. Dunnwald, K.A. Krohn, D.A. Mankoff, Quantitative fluoroestradiol positron emission tomography imaging predicts response to endocrine treatment in breast cancer, J. Clin. Oncol. 24 (18) (2006) 2793–2799.

[27] C.M. Venema, L.H. Mammatas, C.P. Schroder, M. van Kruchten, G. Apollonio, A. Glaudemans, A.H.H. Bongaerts, O.S. Hoekstra, H.M.W. Verheul, E. Boven, B. van der Vegt, E.F.J. de Vries, E.G.E. de Vries, R. Boellaard, C.W. Menke van der Houven van Oordt, G.A.P. Hospers, Androgen and estrogen receptor imaging in metastatic breast cancer patients as a surrogate for tissue biopsies, J. Nucl. Med. 58 (12) (2017) 1906–1912.

[28] S.Y. Chae, S.B. Kim, S.H. Ahn, H.O. Kim, D.H. Yoon, J.H. Ahn, K.H. Jung, S. Han, S. J. Oh, S.J. Lee, H.J. Kim, B.H. Son, G. Gong, H.S. Lee, D.H. Moon, A randomized feasibility study of (18)F-fluoroestradiol PET to predict pathologic response to neoadjuvant therapy in estrogen receptor-rich postmenopausal breast cancer, J. Nucl. Med. 58 (4) (2017) 563–568.

[29] C. Liu, C. Gong, S. Liu, Y. Zhang, Y. Zhang, X. Xu, H. Yuan, B. Wang, Z. Yang, (18)F-FES PET/CT influences the staging and management of patients with newly diagnosed estrogen receptor-positive breast cancer: a retrospective comparative study with (18)F-FDG PET/CT, Oncologist 24 (12) (2019) e1277–e1285.

[30] E. Currin, L.M. Peterson, E.K. Schubert, J.M. Link, K.A. Krohn, R.B. Livingston, D. A. Mankoff, H.M. Linden, Temporal heterogeneity of estrogen receptor expression in bone-dominant breast cancer: 18f-fluoroestradiol PET imaging shows return of ER expression, J. Compr. Canc. Netw. 14 (2) (2016) 144–147.